Inorganic Chemistry

Article

pubs.acs.org/IC

Enhancement of Cytotoxicity by Combining Pyrenyl-Dendrimers and Arene Ruthenium Metallacages

Anaïs Pitto-Barry,[†] Olivier Zava,[‡] Paul J. Dyson,[‡] Robert Deschenaux,[†] and Bruno Therrien*[,†]

[†]Institut de Chimie, Université de Neuchâtel, Avenue de Bellevaux 51, CH-2000 Neuchâtel, Switzerland

[‡]Institut des Sciences et Ingénierie Chimique, Ecole Polytechnique Fédérale de Lausanne (EPFL), CH-1015 Lausanne, Switzerland

Supporting Information

ABSTRACT: Three generations of pyrenyl bis-MPA dendrimers with two different end-groups, acetonide (pyr_{Gn}) or alcohol ($pyr_{Gn\text{-}OH}$) (n = 1−3), were synthesized, and the pyrenyl group of the dendritic molecules was encapsulated in the arene ruthenium metallacages, $[Ru_6(p\text{-cymene})_6(OO{\cap}OO)_3(tpt)_2]^{6+}$ ($OO{\cap}OO$ = 5,8-dioxydo-1,4-naphtaquinonato (donq) $[\mathbf{1}]^{6+}$ and 6,11-dioxydo-5,12-naphtacenedionato (dotq) $[\mathbf{2}]^{6+}$; tpt =2,4,6-tri(pyridin-4-yl)-1,3,5-triazine). The host−guest properties of $[guest{\subset}\mathbf{1}]^{6+}$ and $[guest{\subset}\mathbf{2}]^{6+}$ were studied in solution by NMR and UV−vis spectroscopic methods, thus allowing the determination of the affinity constants. Moreover, the cytotoxicity of these water-soluble host−guest systems and the pyrenyl-dendrimers was evaluated on human ovarian cancer cells.

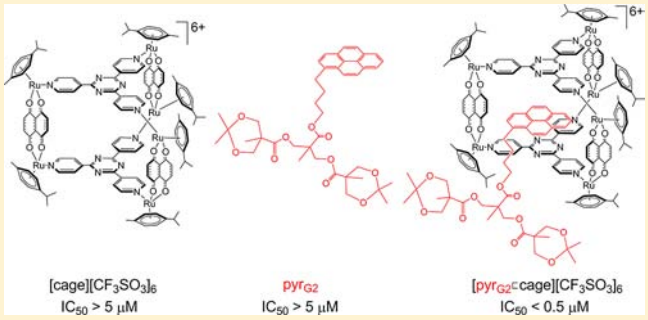

INTRODUCTION

The synthesis of dendrimers with defined structures is now well established,[1] employing divergent,[2] convergent,[3] and the somewhat less exploited double-stage convergent[4] routes. Since these routes allow dendrimers to be prepared with precise sizes and shapes, and since dendrimers are relatively easy to functionalize,[5] and possess other interesting properties,[6] they have been studied as potential drug delivery vectors. Water-soluble dendrimers have been shown to improve drug solubility, increase drug circulation time, and prolong drug residence in tumors, thus reducing toxicity.[7] Biodegradability is an important criteria in order to avoid cellular accumulation leading to lysosomal storage disease in patients.[8] Most dendrimers are based on ester or amide linkages which degrade by chemical hydrolysis or enzymatic cleavage under physiological conditions.[9] Some dendrimers are both water-soluble and biodegradable such as poly(2,2-bis(hydroxymethyl)-propionic acids (bisMPA),[10] poly(L-lysine) dendrimers (PLL),[11] polyester structures (PGLSA−OH),[12] and polyamidoamine derivatives (PAMAM),[2b] among others.[13] For example, a fourth generation polyester dendron attached to a trisphenolic core derived from the monomeric unit bis-MPA has been evaluated for drug delivery applications.[14] Cell proliferation studies have suggested that the dendritic scaffold did not exhibit a significant toxic effect. The attachment of poly(ethylene glycol) to the surface of this type of dendrimer has also been successful for therapeutic applications,[10b,15] and structure−activity relationships have shown that both generation and steric effect are important.[7]

Recently, we have reported the synthesis of host−guest systems composed of water-soluble arene ruthenium metallaprisms and pyrenyl-functionalized dendrimers.[16] In these systems, assessment of the biological activity of the pyrenyl-functionalized dendrimers was not possible due to their hydrophobic nature, and consequently, only the antiproliferative activity of the host−guest systems was evaluated. These studies showed that the host−guest systems inhibit the growth of both sensitive and cisplatin resistant cancer cells (A2780 and A2780cisR) with IC_{50} values comparable to those of the empty metallaprisms, thus questioning the role of the dendritic appendages in these systems. Therefore, to determine if a dendritic effect can be obtained by combining functionalized-dendrimer and metallacage, water-soluble dendrimers are necessary.

Herein we present the synthesis of different generations of biodegradable water-soluble dendrimers based on the bis-MPA monomer unit functionalized by a pyrenyl unit. The aromatic part of the pyrenyl-functionalized dendrimers may be encapsulated into the hydrophobic cavity of the hexanuclear arene ruthenium metallacages $[Ru_6(p\text{-cymene})_6(OO{\cap}OO)_3(tpt)_2]^{6+}$ ($OO{\cap}OO$ = 5,8-dioxydo-1,4-naphtaquinonato (donq) $[\mathbf{1}]^{6+}$, 6,11-dioxydo-5,12-naphtacenedionato (dotq) $[\mathbf{2}]^{6+}$; tpt =2,4,6-tri(pyridin-4-yl)-1,3,5-triazine).[17] In contrast to the previously reported pyrenyl-dendrimers in metallaprism $[\mathbf{1}]^{6+}$,[16] the biological activity of both the dendrimers and of the host−guest systems has been evaluated. The cytotoxicity of the resulting host−guest systems is considerably greater than that of the individual hosts and guests.

Received: December 21, 2011
Published: June 20, 2012

   dx.doi.org/10.1021/ic202739d | *Inorg. Chem.* 2012, 51, 7119−7124

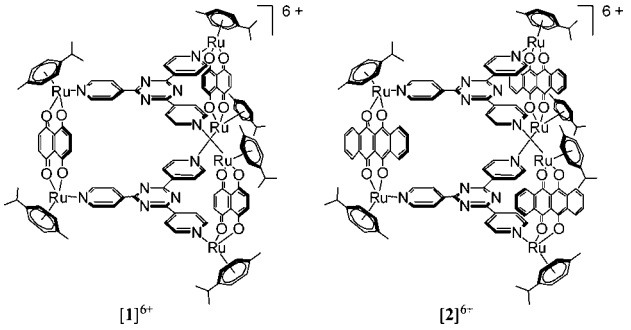

[1]$^{6+}$ [2]$^{6+}$

RESULTS AND DISCUSSION

Three generations of pyrenyl bis-MPA dendrimers with acetonide (pyr_{Gn}) or alcohol ($pyr_{Gn\text{-}OH}$) (n = 1−3) end-groups were prepared by two routes (Scheme 1). In the first approach, 1-pyrenebutanol reacts with acetonide-2,2-bis(methoxy)-propionic acid (AMP) to give the first generation pyr_{G1} dendrimer which is then deprotected to obtain $pyr_{G1\text{-}OH}$. The same sequence of reactions is used to synthesize the second and third generation dendrons from the corresponding pyrenyl-dendritic intermediates. Alternatively, pyr_{G2} and pyr_{G3} can also be synthesized from the bis-MPA dendrimers[18] acetonide-Gn-CO_2H (n = 2−3) (bearing a carboxylic group at the focal point and acetonide groups at the periphery) via esterification with 1-pyrenebutanol. Finally, to obtain the third generation pyr_{G3} another approach is also used: the previously synthesized $pyr_{G1\text{-}OH}$ and acetonide-G2-CO_2H react together via esterification. This method allows a better yield in the last step. All the esterifications have been performed using *N,N′*-dicyclohexylcarbodiimide (DCC) as coupling agent and 4-(dimethylamino)pyridinium *p*-toluene sulfonate (DPTS) as catalyst.[19] Deprotection of the acetonide was performed with an acidic resin in methanol as previously described.[18] The first method is preferable as it involved 7 steps (Scheme 1), while the convergent approach[18] requires 13 steps (see Supporting Information). Nevertheless, both methods can be used to prepare these three generations of pyrenyl-dendrimers.

The esterification reaction with 1-pyrenebutanol was monitored by ^{1}H NMR spectroscopy. The signals of the aliphatic protons of the pyrenyl part are shifted slightly upfield after coupling (by up to 0.05 ppm relative to the reactant). Accordingly, for the divergent approach (the synthesis of pyr_{Gn} from $pyr_{G(n\text{-}1)\text{-}OH}$), the methyl resonances (singlets) are shifted downfield (by up to 0.1 ppm relative to the previous generation) as the generation increases with an increase in their relative integration ratio. Deprotection of the alcohol groups was also observed by ^{1}H NMR spectroscopy with the disappearance of the acetonide signals. In addition, the ^{1}H NMR spectra of the different pyrenyl derivatives pyr_{Gn} reveal the influence of the carbonyl group on the two β methyl groups attached to the external generation; the methyl resonance results in two doublets. The proton, H_a, located near the ester group shifts downfield by up to 0.5 ppm relative to proton H_b, which is less affected by this influence. Interestingly, the methyl protons of the inner generations do not show this behavior (Figure 1). These differences can also be seen for the alcohol free pyrenyl derivatives ($pyr_{Gn\text{-}OH}$).

The inclusion complexes [guest⊂**1**]$^{6+}$ and [guest⊂**2**]$^{6+}$ were prepared in two steps (Scheme 2). The dinuclear complexes, $[Ru_2(p\text{-cymene})_2(donq)Cl_2]$ or $[Ru_2(p\text{-cymene})_2(dotq)Cl_2]$, are first reacted with $AgCF_3SO_3$ to afford a dinuclear intermediate (not isolated), and then 2 equiv of the tpt panels and 1 equiv of the guest molecule (pyr_{Gn} and $pyr_{Gn\text{-}OH}$) are added to obtain the corresponding inclusion compound. The resulting hexacationic host−guest systems are isolated in ca. 70% yield as their triflate salts $[guest⊂\mathbf{1}][CF_3SO_3]_6$ and $[guest⊂\mathbf{2}][CF_3SO_3]_6$.

The host−guest properties of [guest⊂**1**]$^{6+}$ and [guest⊂**2**]$^{6+}$ have been studied in solution. Their stability in a mixture of water and DMSO (20/80 v/v) was established at room and elevated temperatures (40 °C). Under these conditions there are no signs of degradation of the cage, or leaching of the guest over 24 h, consistent with previous observations.[20] Diffusion-ordered NMR spectroscopy (DOSY) measurements in pure DMSO, at room temperature, were also performed. As an example, the DOSY spectra of [**1**]$^{6+}$ and [$pyr_{G2\text{-}OH}$⊂**1**]$^{6+}$ give

Scheme 1. Synthesis of the Pyrenyl Bis-MPA Dendrimers[a]

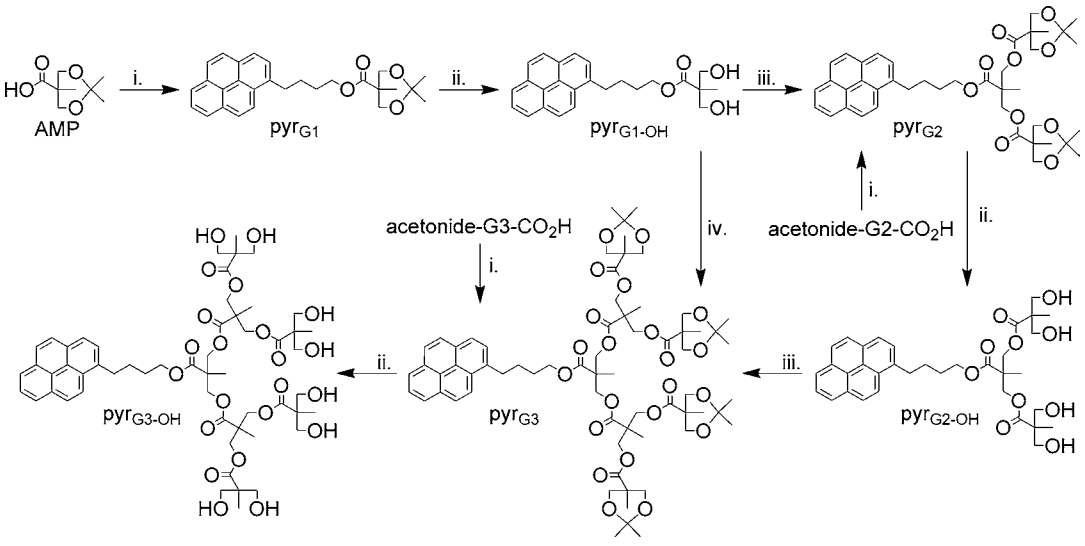

[a](i) 1-Pyrenebutanol, DCC, DPTS, dry CH_2Cl_2; (ii) Dowex H+, MeOH; (iii) AMP, DCC, DPTS, dry CH_2Cl_2; (iv) acetonide-G2-CO_2H, DCC, DPTS, dry CH_2Cl_2.

dx.doi.org/10.1021/ic202739d | Inorg. Chem. 2012, 51, 7119−7124

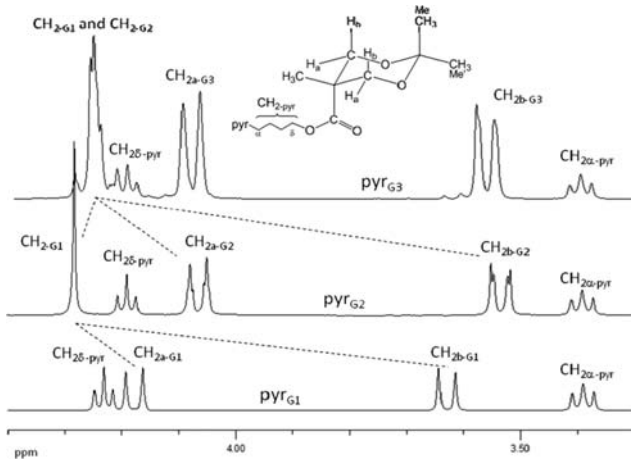

Figure 1. NMR spectra showing the aliphatic protons of pyr_{Gn} (n = 1–3) (in CD_2Cl_2, 23 °C).

Scheme 2. Encapsulation of Guest in the Metallaprism $[\mathbf{1}]^{6+}$

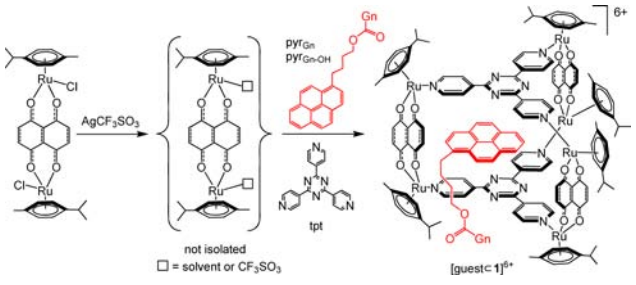

almost equivalent diffusion coefficients (D) with values at ca. 6.3×10^{-10} $m^2 \cdot s^{-1}$, thus suggesting the encapsulation of $pyr_{G2\text{-}OH}$ in the hydrophobic cavity of $[\mathbf{1}]^{6+}$ and the formation of a $[pyr_{G2\text{-}OH}\subset\mathbf{1}]^{6+}$ adduct, see Figure 2. The DOSY spectrum

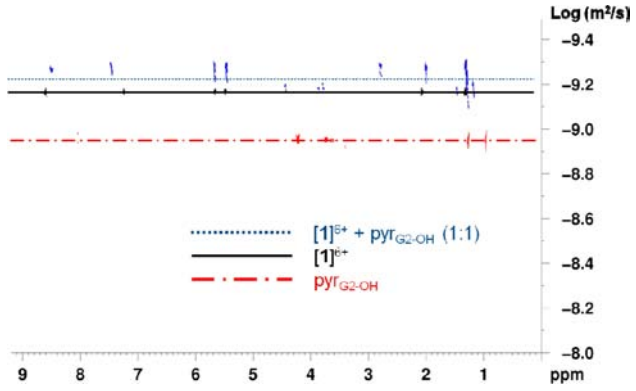

Figure 2. DOSY spectra of $pyr_{G2\text{-}OH}$, $[\mathbf{1}]^{6+}$ and $[pyr_{G2\text{-}OH}\subset\mathbf{1}]^{6+}$ in DMSO at room temperature.

of free pyr_{G2OH} is also shown in Figure 2, and a diffusion coefficient of 0.13×10^{-10} $m^2 \cdot s^{-1}$ was estimated, which confirms the entrapment of the guest molecule in $[\mathbf{1}]^{6+}$. Similar results were obtained with the metallaprism $[\mathbf{2}]^{6+}$ and the corresponding $[guest\subset\mathbf{2}]^{6+}$ systems. All diffusion coefficients of the host–guest systems are listed in Table 1.

The stability constants of association (K_a) for these host–guest systems were estimated by UV–vis titrations of the pyrenyl derivatives in the presence of the cages at room temperature in CH_2Cl_2 or DMSO depending on the solubility

Table 1. Diffusion Coefficients Obtained from the DOSY NMR Spectra and Association Constants of Pyrenyl-Containing Dendrimers Estimated from UV–Vis Titrations (CH_2Cl_2 or DMSO at 21 °C)

compd	log D DMSO	K_a (10^4 M^{-1}) CH_2Cl_2	K_a (10^4 M^{-1}) DMSO
$[pyr_{G1}\subset\mathbf{1}][CF_3SO_3]_6$	−9.3	9.5	n.d.
$[pyr_{G2}\subset\mathbf{1}][CF_3SO_3]_6$	−9.1	1.5	n.d.
$[pyr_{G3}\subset\mathbf{1}][CF_3SO_3]_6$	−9.3	13.1	n.d.
$[pyr_{G1\text{-}OH}\subset\mathbf{1}][CF_3SO_3]_6$	−9.3	0.5	0.5
$[pyr_{G2\text{-}OH}\subset\mathbf{1}][CF_3SO_3]_6$	−9.2	n.d.	0.6
$[pyr_{G3\text{-}OH}\subset\mathbf{1}][CF_3SO_3]_6$	−9.8	n.d.	0.6
$[pyr_{G1}\subset\mathbf{2}][CF_3SO_3]_6$	−10.1	2.0	0.4
$[pyr_{G2}\subset\mathbf{2}][CF_3SO_3]_6$	−10.1	0.5	n.d.
$[pyr_{G3}\subset\mathbf{2}][CF_3SO_3]_6$	−10.1	0.2	n.d.
$[pyr_{G1\text{-}OH}\subset\mathbf{2}][CF_3SO_3]_6$	−10.1	9.6	1.7
$[pyr_{G2\text{-}OH}\subset\mathbf{2}][CF_3SO_3]_6$	−10.1	n.d.	3.3
$[pyr_{G3\text{-}OH}\subset\mathbf{2}][CF_3SO_3]_6$	−10.1	n.d.	6.2

of the dendrimers. The K_a values (Table 1) were obtained using a nonlinear least-squares fitting method.[21] The association constants are quite high and support the encapsulation of the guest within the host, which is consistent with the DOSY measurements. Moreover, these values are comparable with those obtained with other pyrenyl-functionalized dendrimers encapsulated by $[\mathbf{1}]^{6+}$.[16]

The stability of the systems was also evaluated under biologically relevant conditions using UV–vis spectroscopy. Absorption spectra of selected $[guest\subset\mathbf{1}]^{6+}$ and $[guest\subset\mathbf{2}]^{6+}$ systems (see Supporting Information) were monitored in a solution of aqueous RPMI 1640 media (Roswell Park Memorial Institute medium) containing GlutaMAX (L-glutamine, folic acid, and $NaHCO_3$). All systems were stable for several hours at 40 °C, with no spectral changes observed. However, after ~12 h the intensity of the absorption band slowly starts to weaken, suggesting partial leakage of the guest and breakage of the cage, and consequently affording smaller fragments in solution. Similar stability was found with analogous pyrenyl-dendrimers[16] and pyrenyl-functionalized[22] molecules encapsulated by $[\mathbf{1}]^{6+}$ and $[\mathbf{2}]^{6+}$. In addition, UV–vis titrations in RPMI 1640 media of some pyrenyl derivatives in the presence of the cages were performed to determine their stability constants of association (see Supporting Information). The K_a values are smaller than those found in CH_2Cl_2 or DMSO (Table 1), but support the idea of having intact host–guest systems under physiological conditions.

Electronic absorption spectra of the pyrenyl derivatives and of the inclusion complexes $[guest\subset\mathbf{1}]^{6+}$ and $[guest\subset\mathbf{2}]^{6+}$ were acquired in the range 200–800 nm in DMSO at 10^{-4} M concentration. The UV–vis spectra of the pyrenyl derivatives are dominated by the absorption of the pyrenyl part (with four characteristic bands between 290 and 390 nm),[23] whereas the host–guest complexes are characterized by an intense high-energy band centered at 260 nm and by an absorption band at around 450 nm assigned to metal-to-ligand charge transfer process (MLCT).[24] The bands observed between 500 and 700 nm are due to the quinonato linkers of the metallaclips.[25] Figure 3 illustrates these electronic absorptions with the spectra of the $[guest\subset\mathbf{1}]^{6+}$ systems. Interestingly, the four characteristic bands of the pyrenyl part found in the region 290–390 nm are much stronger in the encapsulated systems than in the spectra of the free pyrenyl derivatives. For example, the molar

dx.doi.org/10.1021/ic202739d | Inorg. Chem. 2012, 51, 7119–7124

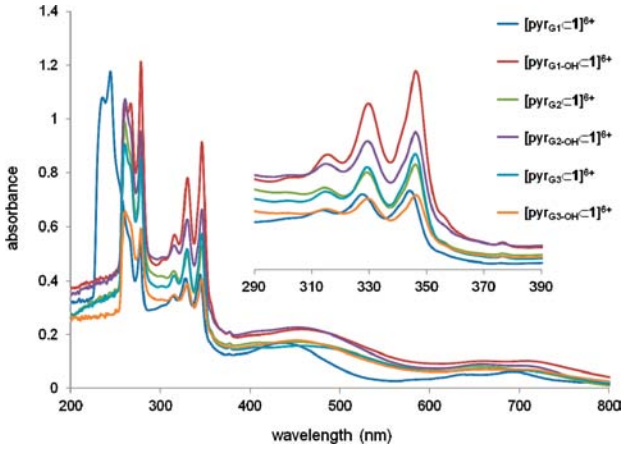

Figure 3. UV−vis spectra of inclusion system [guest⊂**1**][CF_3SO_3]$_6$ in DMSO (10^{-4} M concentration).

extinction coefficient of the pyrenyl band of free $pyr_{G3\text{-}OH}$ at 316 nm is found at 10 700 L·mol^{-1}·cm^{-1} and at 34 000 L·mol^{-1}·cm^{-1} in $[pyr_{G3\text{-}OH}\subset\mathbf{1}]^{6+}$. This increase of the molar extinction coefficients of the pyrenyl bands is typical of host−guest pyrene-containing systems[26] and clearly indicates a synergic effect of the electronic absorptions due to the association of metallaprisms and pyrenyl derivatives.

Under the conditions of electrospray ionization mass spectrometry (ESI-MS), the $[guest\subset\mathbf{1}]^{6+}$ and $[guest\subset\mathbf{2}]^{6+}$ systems are remarkably stable. Along with fragmentation peaks ($[\{Ru_2(p\text{-cymene})_2(OO\cap OO)\} - 2Cl + CF_3SO_3]^+$ and $[\{Ru_2(p\text{-cymene})_2(OO\cap OO)\} - 2Cl + tpt + CF_3SO_3]^+$), the peak envelopes of $[guest + \mathbf{1} + 3CF_3SO_3]^{3+}$ and of $[guest + \mathbf{2} + 3CF_3SO_3]^{3+}$ are found for all inclusion systems. These peaks are assigned unambiguously on the basis of their characteristic Ru_6 isotope pattern and confirm the stability of these host−guest systems. The ESI-MS spectrum of $[pyr_{G2\text{-}OH}\subset\mathbf{2}][CF_3SO_3]_6$ is shown in Figure 4. A peak envelope corresponding to $[pyr_{G2\text{-}OH} + \mathbf{2} + 3CF_3SO_3]^{3+}$ is observed at m/z 1323.54, with fragmentation peaks corresponding to $[\{Ru_2(p\text{-cymene})_2(dotq)\} - 2Cl + CF_3SO_3]^+$ and $[\{Ru_2(p\text{-cymene})_2(dotq)\} - 2Cl + tpt + CF_3SO_3]^+$ observed at m/z 908.06 and 1221.15, respectively.

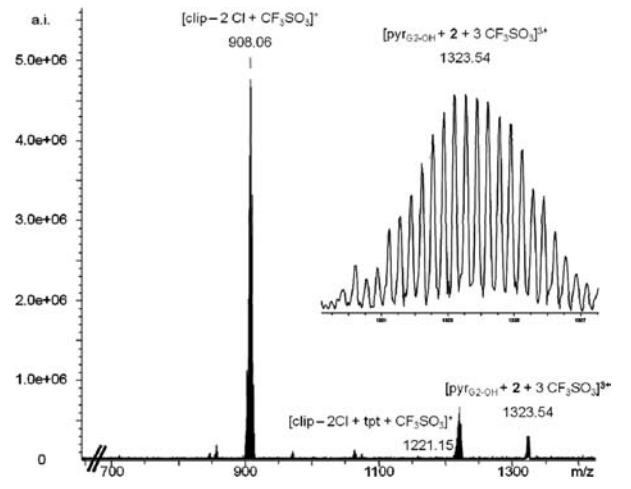

Figure 4. ESI-MS spectrum of inclusion system $[pyr_{G2\text{-}OH}\subset\mathbf{2}][CF_3SO_3]_6$ in MeOH with fragmentations and peak envelope of $[pyr_{G2\text{-}OH} + 2 + 3CF_3SO_3]^{3+}$ (clip = $\{Ru_2(p\text{-cymene})_2(dotq)\}$).

Chem3D simulations,[27] used to gain some structural information, show the dendritic arm extending from the metallaprism with the pyrenyl moiety being encapsulated inside the cavity (Figure 5). The $[pyr_{G1}\subset\mathbf{2}]^{6+}$, $[pyr_{G2}\subset\mathbf{2}]^{6+}$, and $[pyr_{G3}\subset\mathbf{2}]^{6+}$ systems are all estimated to be approximately 4 nm in length, despite the presence of different generations of the dendritic arm. This observation is consistent with the diffusion coefficients which show similar diffusion coefficient for all host−guest systems.

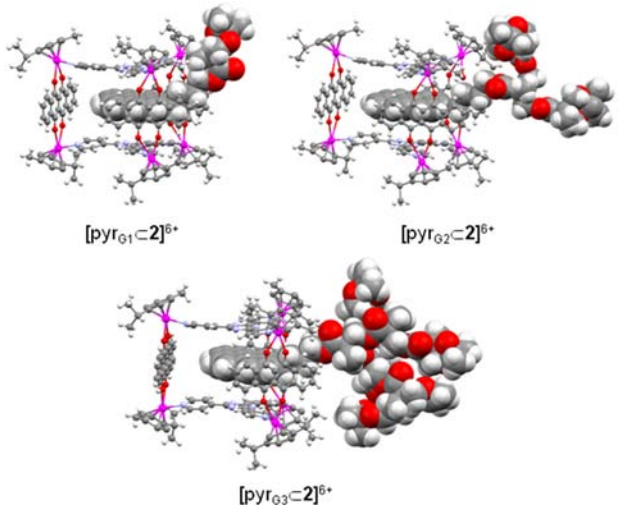

Figure 5. Simulations of $[pyr_{G1}\subset\mathbf{2}]^{6+}$, $[pyr_{G2}\subset\mathbf{2}]^{6+}$, and $[pyr_{G3}\subset\mathbf{2}]^{6+}$ systems.

The antiproliferative activity of the pyrenyl-containing dendrimers pyr_{Gn} and $pyr_{Gn\text{-}OH}$, complexes $[\mathbf{1}][CF_3SO_3]_6$ and $[\mathbf{2}][CF_3SO_3]_6$, and the host−guest systems $[pyr_{Gn}\subset\mathbf{1}][CF_3SO_3]_6$, $[pyr_{Gn\text{-}OH}\subset\mathbf{1}][CF_3SO_3]_6$, $[pyr_{Gn}\subset\mathbf{2}][CF_3SO_3]_6$, and $[pyr_{Gn\text{-}OH}\subset\mathbf{2}][CF_3SO_3]_6$ were evaluated against human ovarian A2780 (cisplatin sensitive) and A2780cisR (acquired resistance to cisplatin) cancer cell lines. Their cytotoxicities, in comparison to cisplatin, are presented in Table 2.

The nature of the terminal group influences the water-solubility of the dendrimers, thus influencing the cytotoxicity of the functionalized-pyrenyl dendrimers, with $pyr_{G2\text{-}OH}$ and $pyr_{G3\text{-}OH}$ showing significant cytotoxicities, comparable to cisplatin, whereas the others, notably the acetonide counterparts, are not cytotoxic, presumably due to their poor solubility in the culture medium. This inactivity of the acetonide functionalized-pyrenyl dendrimers suggests that, despite a limited stability over a 72 h period, the decomposition products formed under biological conditions are not cytotoxic. It is also worth mentioning that the cytotoxicities on both cisplatin resistant and cisplatin sensitive cancer cell lines are almost equivalent for all compounds tested, suggesting a mode of action and/or detoxification different from cisplatin. Overall, the pyrenyl derivatives encapsulated within $[\mathbf{1}]^{6+}$ are slightly more toxic than their analogues entrapped in $[\mathbf{2}]^{6+}$.

In contrast with the pyrenyl-functionalized poly(aryl ester) containing cyanobiphenyl groups[16a] and the pyrenyl poly(benzyl ether) containing flexible chains[16b] encapsulated by $[\mathbf{1}]^{6+}$, the cytotoxicity of the $[guest\subset\mathbf{cage}]^{6+}$ systems are not equivalent to the cytotoxicity of the empty cages. Indeed, the hexaruthenium hosts $[\mathbf{1}]^{6+}$ and $[\mathbf{2}]^{6+}$ exhibit similar cytotox-

dx.doi.org/10.1021/ic202739d | Inorg. Chem. 2012, 51, 7119−7124

Table 2. IC_{50} Values with Standard Deviations of Pyrenyl-Containing Dendrimers, Empty Metallaprisms, and Host–Guest Systems on A2780 and A2780cisR Cell Lines

compd	A2780 (IC_{50} [μM])	A2780cisR (IC_{50} [μM])
pyr_{G1}	n.d.	n.d.
pyr_{G2}	n.d.	n.d.
pyr_{G3}	n.d.	n.d.
$pyr_{G1\text{-}OH}$	n.d.	n.d.
$pyr_{G2\text{-}OH}$	5.9 ± 0.6	7.4 ± 0.8
$pyr_{G3\text{-}OH}$	8.7 ± 0.9	8.7 ± 1.0
[**1**][CF_3SO_3]$_6$	3.1 ± 1.0	4.6 ± 0.5
[**2**][CF_3SO_3]$_6$	4.1 ± 0.07	6.5 ± 1.0
[pyr_{G1}⊂**1**][CF_3SO_3]$_6$	1.2 ± 0.1	0.9 ± 0.08
[pyr_{G2}⊂**1**][CF_3SO_3]$_6$	0.3 ± 0.02	0.2 ± 0.02
[pyr_{G3}⊂**1**][CF_3SO_3]$_6$	0.7 ± 0.3	0.8 ± 0.2
[$pyr_{G1\text{-}OH}$⊂**1**][CF_3SO_3]$_6$	1.4 ± 0.1	0.9 ± 0.08
[$pyr_{G2\text{-}OH}$⊂**1**][CF_3SO_3]$_6$	2.0 ± 0.5	1.3 ± 0.4
[$pyr_{G3\text{-}OH}$⊂**1**][CF_3SO_3]$_6$	0.7 ± 0.1	0.8 ± 0.1
[pyr_{G1}⊂**2**][CF_3SO_3]$_6$	2.1 ± 0.4	1.6 ± 0.2
[pyr_{G2}⊂**2**][CF_3SO_3]$_6$	1.9 ± 0.4	0.9 ± 0.3
[pyr_{G3}⊂**2**][CF_3SO_3]$_6$	1.1 ± 0.3	1.5 ± 0.4
[$pyr_{G1\text{-}OH}$⊂**2**][CF_3SO_3]$_6$	0.8 ± 0.3	2.2 ± 0.8
[$pyr_{G2\text{-}OH}$⊂**2**][CF_3SO_3]$_6$	4.1 ± 0.6	1.9 ± 0.3
[$pyr_{G3\text{-}OH}$⊂**2**][CF_3SO_3]$_6$	1.5 ± 0.03	1.5 ± 0.4
cisplatin	1.6 ± 0.6	8.6 ± 0.6

icities to $pyr_{G2\text{-}OH}$ and $pyr_{G3\text{-}OH}$, and remarkably, when combined, the resulting host–guest systems are significantly more active than either the host or the guest alone. This difference is especially noticeable with [$pyr_{G3\text{-}OH}$⊂**2**][CF_3SO_3]$_6$, which shows individual IC_{50} values of 8.7 μM for $pyr_{G3\text{-}OH}$ and 6.5 μM for [**2**][CF_3SO_3]$_6$ on A2780cisR cells, while the IC_{50} value for the host–guest system [$pyr_{G3\text{-}OH}$⊂**2**][CF_3SO_3]$_6$ is 0.8 μM. The enhanced cytotoxicity of the [guest⊂**cage**]$^{6+}$ systems compared to the guest or host alone implies that intact [guest⊂**cage**]$^{6+}$ systems are entering the cells together, and are responsible for the overall cytotoxicity observed.

CONCLUSION

In summary, the entrapment of water-soluble dendrimer guests within metallaprism hosts leads to apparent enhancements in cytotoxicity. The host–guest system is also quite stable in biological media. These features, combined with their potential to preferentially accumulate in tumors, make them interesting candidates for further study and development.

ASSOCIATED CONTENT

Supporting Information

General information, detailed syntheses, and analytical data of all the pyrenyl-dendrimers and the corresponding host–guest systems. NMR spectra of all compounds and UV–vis titrations under biologically relevant conditions. This material is available free of charge via the Internet at http://pubs.acs.org.

AUTHOR INFORMATION

Corresponding Author

*E-mail: bruno.therrien@unine.ch. Fax: (+) 41 32 7182511.

Notes

The authors declare no competing financial interest.

ACKNOWLEDGMENTS

R.D. thanks the Swiss National Science Foundation for financial support (Grant 200020-129501). A.P.-B. thanks Dr. R. A. Slobodeanu and Dr. N. P. E. Barry for their help. A generous loan of $RuCl_3 \cdot nH_2O$ from Johnson Matthey Technology Centre is gratefully acknowledged.

REFERENCES

(1) Carlmark, A.; Hawker, C. J.; Hult, A.; Malkoch, M. *Chem. Soc. Rev.* **2009**, *38*, 352–362.
(2) (a) Buhleier, E.; Wehner, W.; Voegtle, F. *Synthesis* **1978**, *2*, 155–158. (b) Tomalia, D. A.; Baker, H.; Dewald, J.; Hall, M.; Kallos, G.; Martin, S.; Roeck, J.; Ryder, J.; Smith, P. *Polym. J.* **1985**, *17*, 117–132. (c) Newkome, G. R.; Yao, Z.; Baker, G. R.; Gupta, V. K. *J. Org. Chem.* **1985**, *50*, 2003–2004.
(3) (a) Hawker, C. J.; Fréchet, J. M. J. *J. Am. Chem. Soc.* **1990**, *112*, 7638–7647. (b) Grayson, S. M.; Fréchet, J. M. J. *Chem. Rev.* **2001**, *101*, 3819–3867.
(4) Wooley, K. L.; Hawker, C. J.; Fréchet, J. M. J. *J. Am. Chem. Soc.* **1991**, *113*, 4252–4261.
(5) (a) Lee, C. C.; MacKay, J. A.; Fréchet, J. M. J.; Szoka, F. C. *Nat. Biotechnol.* **2005**, *23*, 1517–1526. (b) Röglin, L.; Lempens, E. H. M.; Meijer, E. W. *Angew. Chem., Int. Ed.* **2010**, *49*, 2–13. (c) Astruc, D.; Boisselier, E.; Ornelas, C. *Chem. Rev.* **2010**, *110*, 1857–1959. (d) Cheng, Y.; Zhao, L.; Li, Y.; Xu, T. *Chem. Soc. Rev.* **2011**, *40*, 2673–2703.
(6) Hourani, R.; Kakkar, A. *Macromol. Rapid Commun.* **2010**, *31*, 947–974.
(7) Fox, M. E.; Szoka, F. C.; Fréchet, J. M. J. *Acc. Chem. Res.* **2009**, *42*, 1141–1151.
(8) Mintzer, M. A.; Grinstaff, M. W. *Chem. Soc. Rev.* **2011**, *40*, 173–190.
(9) Medina, S. H.; El-Sayed, M. E. H. *Chem. Rev.* **2009**, *109*, 3141–3157.
(10) (a) Ihre, H.; Hult, A.; Söderlind, E. *J. Am. Chem. Soc.* **1996**, *118*, 6388–6395. (b) Lee, C. C.; Gillies, E. R.; Fox, M. E.; Guillaudeu, S. J.; Fréchet, J. M. J.; Dy, E. E.; Szoka, F. C. *Proc. Natl. Acad. Sci. U.S.A.* **2006**, *103*, 16649–16654.
(11) Denkewalter, R. G.; Kolc, J. F.; Lukasavage, W. J. U.S. Patent 4289872, 1981.
(12) Carnahan, M. A.; Grinstaff, M. W. *Macromolecules* **2006**, *39*, 609–616.
(13) Rolland, O.; Turrin, C.-O.; Caminade, A.-M.; Majoral, J.-P. *New J. Chem.* **2009**, *33*, 1809–1824.
(14) Padilla de Jésus, O. L.; Ihre, H. R.; Gagne, L.; Fréchet, J. M. J.; Szoka, F. C. *Bioconjugate Chem.* **2002**, *13*, 453–461.
(15) Kojima, C.; Kono, K.; Maruyama, K.; Takagishi, T. *Bioconjugate Chem.* **2000**, *11*, 910–917.
(16) (a) Pitto-Barry, A.; Barry, N. P. E.; Zava, O.; Deschenaux, R.; Dyson, P. J.; Therrien, B. *Chem.—Eur. J.* **2011**, *17*, 1966–1971. (b) Pitto-Barry, A.; Barry, N. P. E.; Zava, O.; Deschenaux, R.; Therrien, B. *Chem.—Asian J.* **2011**, *6*, 1595–1603.
(17) (a) Barry, N. P. E.; Therrien, B. *Eur. J. Inorg. Chem.* **2009**, 4695–4700. (b) Freudenreich, J.; Barry, N. P. E.; Süss-Fink, G.; Therrien, B. *Eur. J. Inorg. Chem.* **2010**, 2400–2405. (c) Schmitt, F.; Freudenreich, J.; Barry, N. P. E.; Juillerat-Jeanneret, L.; Süss-Fink, G.; Therrien, B. *J. Am. Chem. Soc.* **2012**, *134*, 754–757.
(18) (a) Ihre, H.; Hult, A.; Fréchet, J. M. J.; Gitsov, I. *Macromolecules* **1998**, *31*, 4061–4068. (b) Würsch, A.; Möller, M.; Glauser, T.; Lim, L. S.; Voytek, S. B.; Hedrick, J. L.; Frank, C. W.; Hilborn, J. G. *Macromolecules* **2001**, *34*, 6601–6615. (c) Malkoch, M.; Hallman, K.; Lutsenko, S.; Hult, A.; Malmström, E.; Moberg, C. *J. Org. Chem.* **2002**, *67*, 8197–8202.
(19) Moore, J. S.; Stupp, S. I. *Macromolecules* **1990**, *23*, 65–70.
(20) Barry, N. P. E.; Zava, O.; Dyson, P. J.; Therrien, B. *Chem.—Eur. J.* **2011**, *17*, 9669–9677.
(21) Thordarson, P. *Chem. Soc. Rev.* **2011**, *40*, 1305–1323.

(22) Yi, J. W.; Barry, N. P. E.; Furrer, M. A.; Zava, O.; Dyson, P. J.; Therrien, B.; Kim, B. H. *Bioconjugate Chem.* **2012**, *23*, 461−471.
(23) (a) Diring, S.; Camerel, F.; Donnio, B.; Dintzer, T.; Toffanin, S.; Capelli, R.; Muccini, M.; Ziessel, R. *J. Am. Chem. Soc.* **2009**, *131*, 18177−18185. (b) Sagara, Y.; Mutai, T.; Yoshikawa, I.; Araki, K. *J. Am. Chem. Soc.* **2007**, *129*, 1520−1521. (c) Song, J. H.; Sailor, M. J. *J. Am. Chem. Soc.* **1997**, *119*, 7381−7385. (d) Adadurov, A. F.; Gurkalenko, Y. A.; Zhmurin, P. N. *J. Fluoresc.* **2010**, *20*, 315−320.
(24) Freudenreich, J.; Furrer, J.; Süss-Fink, G.; Therrien, B. *Organometallics* **2011**, *30*, 942−951.
(25) Barry, N. P. E.; Furrer, J.; Therrien, B. *Helv. Chim. Acta* **2010**, *93*, 1313−1328.
(26) Colquhoun, H. M.; Zhu, Z.; Williams, D. J.; Drew, M. G. B.; Cardin, C. J.; Gan, Y.; Crawford, A. G.; Marder, T. B. *Chem.—Eur. J.* **2010**, *16*, 907−918.
(27) *Chem3D Pro 11.0 for PC*; CambridgeSoft: Cambridge, MA.